Assessment of GPS Carrier-Phase Stability for Time-Transfer Applications

Kristine M. Larson, Judah Levine, Lisa M. Nelson, *Member, IEEE*, and Thomas E. Parker, *Fellow, IEEE*

Abstract– **We have conducted global positioning system (GPS) carrier-phase time-transfer experiments between the master clock (MC) at the U.S. Naval Observatory (USNO) in Washington, DC and the alternate master clock (AMC) at Schriever Air Force Base near Colorado Springs, Colorado. These clocks are also monitored on an hourly basis with two-way satellite time-transfer (TWSTT) measurements. We compared the performance of the GPS carrier-phase and TWSTT systems over a 236-d period. Because of power problems and data outages during the carrier-phase experiment, the longest continuous time span is 96 d. The data from this period show agreement with TWSTT within ±1 ns, apart from an overall constant time offset (caused by unknown delays in the GPS hardware at both ends). For averaging times of a day, the carrier-phase and TWSTT systems have a frequency uncertainty of 2.5 and 5.5 parts in 10^{15}, respectively.**

I. Introduction

Very accurate frequency- and time-transfer systems will be required to compare cesium fountain primary frequency standards [1]. With that in mind, we have conducted a study of a GPS carrier-phase timing system to assess its long- and short-term stability. Initial analysis of carrier-phase data for time-transfer applications has been extremely promising [2]–[10]. Specifically, comparisons between carrier-phase and code-based common-view GPS show good agreement at times greater than 1 d [2], [4]–[6]. Because both systems depend directly on the GPS constellation, this is not a truly independent measure of the accuracy of GPS carrier-phase time-transfer. Furthermore, the noise of the common-view technique for periods of less than a few days limits the value of comparisons between the common-view and carrier-phase techniques.

In [5], we analyzed 60 d of carrier-phase data collected at the USNO in Washington, D.C. and at the National Institute of Standards and Technology (NIST) in Boulder, Colorado to compare the carrier-phase technique with the TWSTT technique. Unfortunately, the irregular TWSTT observing schedule (no more than three measurements per week) limited our ability to determine the carrier-phase time-transfer stability for intervals less than 1 d. Although agreement between TWSTT and carrier-phase time-transfer over 2 mo was promising, a longer experiment was needed to establish long-term stability. In our current study, we have used the TWSTT system between the MC at USNO and the USNO AMC at Schriever Air Force Base (Colorado Springs, CO). This TWSTT system is both highly precise and makes hourly measurements, providing more frequent measurements than the NIST TWSTT link with USNO. These data allow us:

- to assess stability of the carrier-phase system at periods of less than 1 d,
- to assess stability of the carrier-phase system over 8 mo,
- to determine the importance of the thermal environment on carrier-phase precision, and
- to investigate the potential stability of real-time carrier-phase time-transfer.

II. GPS Carrier-Phase Data Analysis

We use geodetic analysis techniques and geodetic GPS receivers in this time-transfer experiment. Geodetic receivers record both carrier-phase and pseudorange data for all visible satellites at specified intervals. In geodetic analysis, both data types are combined with precise models to estimate relative clock estimates. The sensitivity of each data type to clocks used in the system is easily seen in the observable equations. The carrier-phase $\Delta\phi_r^s$ and pseudorange P_r^s observables for a given satellite s and receiver r are written as

$$-\Delta\phi_r^s\lambda = \rho_g + c\delta^s - c\delta_r + N_r^s\lambda + \rho_t - \rho_i + \rho_{m\phi} + \epsilon_\phi \tag{1}$$

and

$$P_r^s = \rho_g + c\delta^s - c\delta_r + \rho_t + \rho_i + \rho_{mp} + \epsilon_p \tag{2}$$

where λ is the carrier wavelength; ρ_g is the geometric range, defined as $|\vec{X}^s - \vec{X}_r|$; $\vec{X}^s$ is the satellite position at the time of transmission; $\vec{X}_r$ is the receiver position at reception time; δ_r and δ^s are the time of the receiver and satellite clocks, respectively; N_r^s is the carrier-phase ambiguity or bias; ρ_t and ρ_i are the propagation delays caused by the troposphere and ionosphere; $\rho_{m\phi}$ and ρ_{mp} are multipath errors; and ϵ_ϕ and ϵ_p represent unmodeled errors and receiver noise for carrier-phase and pseudorange data, respectively. Included in N_r^s are phase delay terms originating in the receiver and the satellite transmitter.

Each observable depends linearly on the receiver clock. Thus, in principle, these data can be used to compare receiver clocks. There are two important differences between

Manuscript received June 30, 1999; accepted November 5, 1999.

K. M. Larson is with the Department of Aerospace Engineering Sciences, University of Colorado, Boulder, CO 80309 (e-mail:Kristine.Larson@colorado.edu).

J. Levine, L. M. Nelson, and T. E. Parker are with the Time and Frequency Division, National Institute of Standards and Technology, Boulder, CO 80303.

the carrier-phase and pseudorange data that impact time-transfer experiments. First, the carrier-phase data are ambiguous and, to be useful, require the estimation of the carrier-phase ambiguity. The pseudorange data are not ambiguous, but ϵ_p is nearly 100 times larger than ϵ_ϕ. The multipath errors for pseudorange data are also much larger than those observed in carrier-phase data [5]. For many geodetic applications, the ambiguous carrier-phase data are preferred because of their great precision. The geodetic problem is primarily motivated by the need to know station coordinates $\bar{X}_r$, which for a stationary receiver can be averaged over many data epochs, most commonly for 24 h. In a time-transfer experiment, a clock estimate will be made at each data epoch, and so the pseudorange data and their data noise ϵ_p are important for solving the time-transfer problem.

To estimate δ_r from the carrier-phase and pseudorange data, we need to model all the elements in (1) and (2) properly. This requires accurate satellite orbits, station coordinates, and precise transformation parameters between the inertial and terrestrial reference frames, i.e., models of precession, nutation, polar motion, and UT1-UTC. We use GPS satellite orbits computed by the International GPS Service (IGS), which have a radial precision of a few centimeters [11]. The effect of the ionosphere is removed by using an appropriate linear combination of the $L1$ and $L2$ phase data. Variations in the troposphere, motions of station coordinates, and carrier-phase ambiguities are estimated from the data. We do not explicitly model site-specific multipath, but we try to minimize it by discarding all data observed below elevation angles of 15 degrees. A more detailed description of our analysis strategy is given in [5].

Although carrier-phase receivers typically record data at 30-s intervals, we have reduced the data to 6-min intervals to reduce the computational burden. Although, in theory, we require only the data from the two receivers participating in the time-transfer experiment, in practice, we have also used data from Algonquin (Ontario, Canada) to help define the terrestrial reference frame and from Goddard Space Flight Center (Greenbelt, MD) to help resolve carrier-phase ambiguities.

The geodetic software we used to analyze the GPS data (GIPSY; Jet Propulsion Laboratory, California Institute of Technology, Pasadena, CA) is most often used to analyze 24 h of data at a time [12]. It is flexible enough that it can analyze more than that, but we have found that it is not practical to analyze more than 4 d at a time. To ensure continuity, in each batch of data, we include 12 h from the next batch. We then compute an overlap bias, which is the mean of the difference between the two batches over 12 h. All results shown in this paper have this overlap bias removed at the 4-d boundaries. An overall unknown bias remains, related to the fact that we do not have a calibrated system. The 8-mo time series can be analyzed in 24 h on a dual-processor 200-MHz workstation. Nearly one-half of that time is spent on resolution of ambiguities.

III. Description of the Carrier-Phase Time-Transfer Systems

Dual-frequency GPS receivers of geodetic quality have been installed at USNO and Schriever Air Force Base. These particular receivers simultaneously track up to 12 satellites and produce both pseudo range and carrier-phase measurements at 30-s intervals.

The USNO GPS receiver is supplied with an external reference signal of 5-MHz from USNO-MC#3. This clock includes a hydrogen maser and an auxiliary output generator (AOG). Its output is steered to the MC, which is known as USNO-MC#2. This clock is also realized using a hydrogen maser. USNO-MC#2 defines UTC (USNO) and is the reference source for TWSTT.

The Schriever GPS receiver also has an external 5 MHz reference, which is supplied by USNO-AMC#1. This AMC also contains a hydrogen maser and an AOG. It is steered to USNO-MC#2 using the hourly TWSTT data between the AMC and USNO.

To compare the carrier-phase and TWSTT estimates between USNO-MC#2 and USNO-AMC#1, we must know the difference between MC#2 and MC#3 at USNO, because the former is the reference for the TWSTT system there, and the latter drives the GPS carrier-phase receiver. This difference is monitored using a switched/multiplexed time-interval counter. The counter is connected to each of the clocks using a fiber-optic link.

The GPS receivers at USNO and Schriever are part of the IGS network, a cooperative, continuously operating GPS tracking network. The IGS site names for GPS data from USNO and Schriever are USNO and AMCT, respectively. The GPS data are freely available over the Internet and can be accessed through anonymous ftp. Descriptions of all IGS sites and data-archiving procedures can be located at http://igscb.jpl.nasa.gov.

IV. Discussion

This comparison covers a period of nearly 8 mo. During that period, USNO made several changes to the carrier-phase system that improved overall system performance. To make the changes, there were occasional periods when one of the receivers was not operating; one period lasted 9 d. Otherwise, data outages were infrequent with occasional gaps either because the receiver stopped tracking or because the PC that recorded the data failed to work properly. If we ignore the 1-wk period when the Schriever receiver installation was being improved, there was a data loss rate of 3% over the 8-mo period with a total of 528 719 GPS carrier-phase observations. The formal error for the carrier-phase clock estimates are on the order of 125 ps. Recall that the carrier-phase data were analyzed in 4.5-d batches with 12 h of overlap between batches. For completeness, we have plotted overlap biases in Fig. 1. The error bars are defined as the RMS about the overlap bias. Both the mean and the RMS are computed

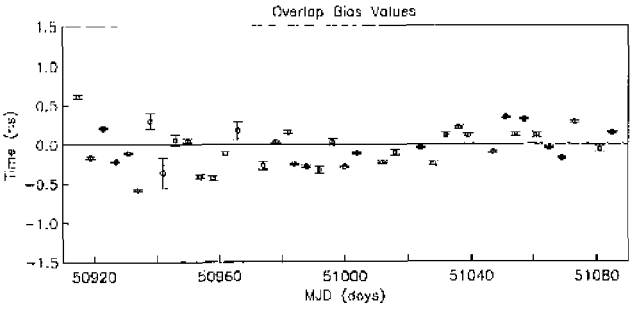

Fig. 1. Overlap bias values computed for periods without data outages and equipment changes. The bias values are the means of the differences over 12 h in two 4.5-d clock solutions. The standard deviations are computed as the RMS about that mean.

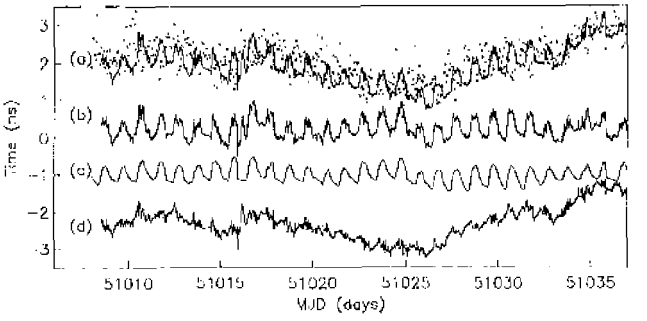

Fig. 2. (a) Carrier-phase clock estimates plotted with TWSTT measurements, (b) data from (a) with low order polynominal removed, (c) local USNO air temperature records converted using 40 ps/°C, and (d) carrier-phase clock estimates with 40 ps/°C temperature correction applied. The time series are offset with respect to each other for display purposes only.

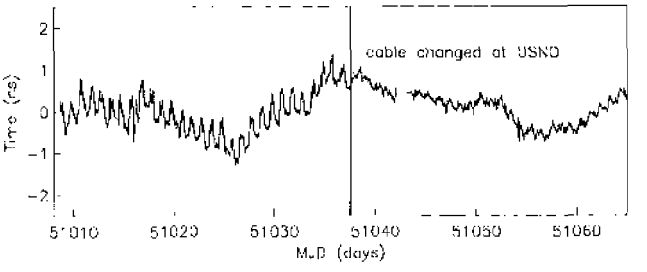

Fig. 3. Carrier-phase estimates of USNO-AMC#1 relative to USNO-MC#2. Note change in diurnal signal apparent after the cable was changed at USNO.

from the overlapping 12-h clock estimates. The overlap biases are due to our analysis strategy, model errors, and data noise. The overlap biases have a mean value of 35 ps, and the RMS scatter about this mean is 222 ps. This indicates that the formal error of 125 ps is at least a factor of two smaller than that observed in the estimates. This is consistent with the results of other geodetic carrier-phase analyses [13].

The TWSTT measurements are made on an hourly basis, with 4367 measurements during this period (an average of about 18 measurements/d). The formal error for an individual TWSTT measurement is generally 225 ps. USNO also computes smooth TWSTT measurements using a Kalman filter. Details about the TWSTT measurement system can be found in [14]. The data from USNO MC#3-MC#2 are made available as hourly measurements [15]. We linearly interpolated these data to compute the correction to the GPS carrier-phase clock estimates.

Because the delays through the GPS receivers were not known, all carrier-phase clock estimates have an unknown time offset with respect to the two-way observations. We have adjusted the mean of the carrier-phase data to compensate for this overall time offset.

V. Cable Delays

In our initial analysis of the carrier-phase clock estimates, we noticed large (peak-to-peak amplitude of ~400 ps) diurnal signals. Comparisons with records at USNO suggested that these periodic signals were highly correlated with local air temperature. The antenna cable used at USNO to connect the antenna to the GPS receiver was 89 m long, and nearly all of it was exposed to the elements. A similar cable was tested and was found to have sensitivity of 0.53 ps/(m-°C). Assuming that 90% of the cable was exposed to a daily temperature variation of 10°C, a cable with this sensitivity to temperature would have a 420-ps p-p diurnal change in its delay. See [16] for more details.

In Fig. 2(a), we show typical carrier-phase clock estimates for the Schriever-USNO baseline. Superimposed on the estimates are the hourly TWSTT measurements, which indicate that the long-term behavior of the carrier-phase estimates is in good agreement with TWSTT. Nevertheless, the diurnal variations in the carrier-phase estimates are readily apparent. In Fig. 2(b), we remove a low order polynomial from the time series so that we can compare more directly with air-temperature records, which are shown in Fig. 2(c), using a conversion factor of 40 ps/°C. In Fig. 2(d), we have subtracted the correction plotted in Fig. 2(d) from the estimates shown in Fig. 2(a), significantly improving the precision of the GPS carrier-phase clock estimates.

Several days after the data shown in Fig. 2 were collected, a new cable was installed at USNO. This cable was expected to a have a temperature sensitivity of less than 0.02 ps/(m-°C) [16]. This new cable was installed in the ceiling of the building instead of on the roof. In Fig. 3, we show carrier-phase clock estimates directly before and after the cable was changed at USNO. It is clear that this new cable has substantially improved the stability of the GPS carrier-phase clock estimates. For the remainder of this paper, all carrier-phase clock estimates will include a 40 ps/°C correction for data collected before the new cable was installed at USNO.

VI. Clock Resets

A previous analysis of data from this particular kind of carrier-phase receiver demonstrated that there were difficulties with the carrier-phase time-transfer system [5]. During this experiment, the AMCT receiver frequently reset its internal clock. This causes a jump in the carrier-phase clock estimates. These resets occur under two circumstances: when the internal clock has drifted by more than 30 ns or when the receiver has recorded a "clock set" command. The first scenario should not be relevant to receivers that are connected to hydrogen masers. The second occurs when power has been turned off or when the receiver has lost track of several satellites, rendering it incapable of determining position. Because position is the primary output of a geodetic receiver, the receiver resets all parameters, including the clock, and searches the sky to re-acquire all visible satellites. Because geodetic GPS receivers were designed to be used by surveyors and geophysicists, it was expected that the units would be used in the field on battery power. Thus, power is frequently turned off. For precise timing applications, power outages must be eliminated as much as possible.

We still do not understand fully why the Schriever receiver reset its clock so frequently. A different receiver of the same model was installed at Schriever in October 1998. The behavior of this receiver was significantly better, with only one reset recorded per 1-mo period. USNO continues to monitor its reset behavior.

It has been proposed that reset calibrations can be computed using the change in the 1-Hz output pulses from the receiver [17]. We were unsure as to the quality of the 1-Hz data, so we originally averaged the clock estimates 30 min before and after each reset to calculate the reset bias [18]. These calculations are only valid if the local reference oscillator is well-behaved during this period. This method is straightforward but is obviously not optimal. It has been noted that clock resets should be multiples of 24.4427-ns, which is one-half of the period of the receiver's internal frequency reference [16]. In Table I, we have compiled all of the reset events that occurred during the study. Using this information, we noticed that of the 18 reset events, 15 of them agree extremely well with the 24.4427 ns increment. For the 15 events, the mean agreement with the theoretical value is 14 ± 85 ps. The other three events are not integer increments of the reference frequency. Upon closer inspection of the AMCT station logs, it was discovered that, in each of these three instances, the operator of the GPS receiver "rebooted" the receiver [19]. In these instances, the reset bias should not be an integer increment of the reference frequency. Because the 1-Hz output depends on the pseudorange data rather than on the carrier-phase, it is unlikely that 1-pps monitoring will be significantly more accurate than using the nearest internal-reference-frequency increment.

TABLE I
Clock Resets

Time MJD	Offset (ns)	Offset/24.4427 (cycles)	Error (ps)	Receiver
50 926.620	195.560	8.001	18	AMCT
50 984.150	−244.345	9.996	82	AMCT
50 997.854	440.083	18.004	114	AMCT
51 000.516	537.716	21.999	−24	USNO
51 002.841	−97.774	4.000	3	AMCT
51 004.304	−48.878	2.000	8	AMCT
51 012.812	195.611	8.003	−69	AMCT
51 016.837	2101.947	85.995	−125	AMCT
51 020.037	−782.158	32.000	8	AMCT
51 047.712	−1026.602	42.000	9	AMCT
51 052.670	−195.518	7.999	24	AMCT
51 061.625	195.541	8.000	0	AMCT
51 065.904*	162.130	6.633	·	AMCT
51 066.508*	180.008	−7.364	·	AMCT
51 070.608*	30.542	−1.249	·	AMCT
51 082.608	97.753	3.999	18	AMCT
51 123.562	−195.373	7.993	168	AMCT
51 129.587	1124.335	45.999	29	AMCT

*Asterisks denote power resets by the station operator.

VII. Data Outages

Unlike the clock resets, for which the data loss is typically small (generally less than 10 min), a lengthy data outage (e.g., caused by a power outage) would produce a bias in the clock estimates that would be difficult to remove because the assumption that the reference oscillator is stable over a long period of time would not be true. For this study, we have not attempted to use the GPS clock estimates themselves to bridge the gaps in the data. Instead, we have used the smoothed TWSTT data as truth, adjusting each carrier-phase segment by a constant time offset with respect to the smooth TWSTT data. In Table II, we have listed the time and length of significant data gaps and associated power outages, with additional information as available.

VIII. Carrier-Phase Noise

In Fig. 4, we display both the individual carrier-phase clock estimates and the TWSTT measurements. Although the TWSTT measurements are noisier than the carrier-phase estimates in the short-term, there is no indication that this is necessarily true in the long term. In Fig. 5, we subtract the carrier-phase estimates from the TWSTT data. The TWSTT-minus-carrier-phase combination gives us an upper bound on the errors in both time-transfer systems.

To investigate the errors in the carrier-phase estimates, we have compared them with the smooth Kalman-filtered TWSTT data. In Fig. 6, we show the difference between the carrier-phase estimates and smooth TWSTT data. Fig. 6 also helps identify which parts of the residuals are carrier-phase error and which are associated with other parts of the time-transfer system. The largest residual is

TABLE II
EXPERIMENT EVENTS.

Time MJD	Receiver	Comments
50 939	USNO	a. 8.4°C spike
51 005	USNO	b. 6.6°C spike
51 007	USNO	c. 22-h data outage
51 014	AMCT	d. 11-h data outage
51 015	USNO	e. 4.5°C spike
51 031	USNO	f. 2.4°C spike
51 037	USNO	g. cable change; thermal chamber installed; data outage
51 042	AMCT	h. 36-h outage
51 098	AMCT	i. 9-d outage; receiver swap/cable problems
51 110	USNO	j. MC steering
51 122	AMCT	k. 24-h outage
51 126	USNO	l. 11°C spike
51 130	USNO	m. roof repairs; 16-h outage
51 133	USNO	n. 9-h outage

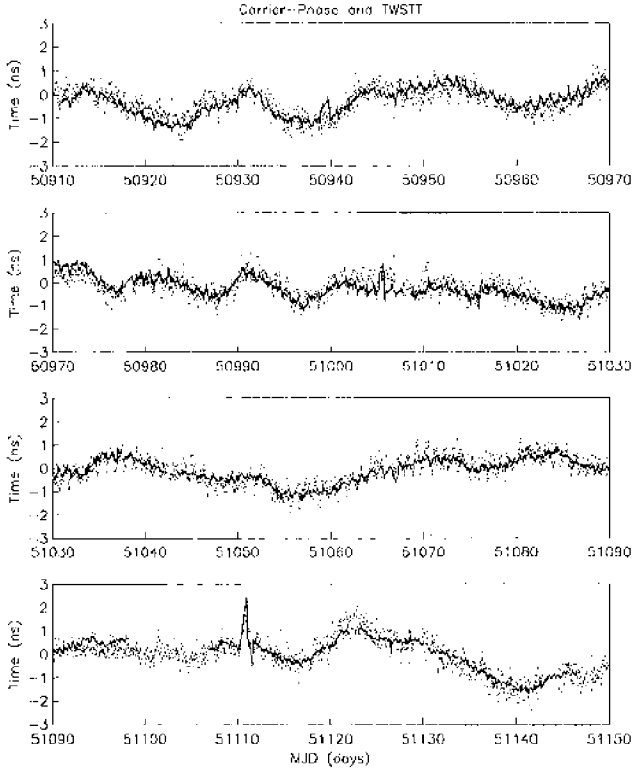

Fig. 4. Carrier-phase clock estimates shown as a line, and individual TWSTT measurements shown as dots.

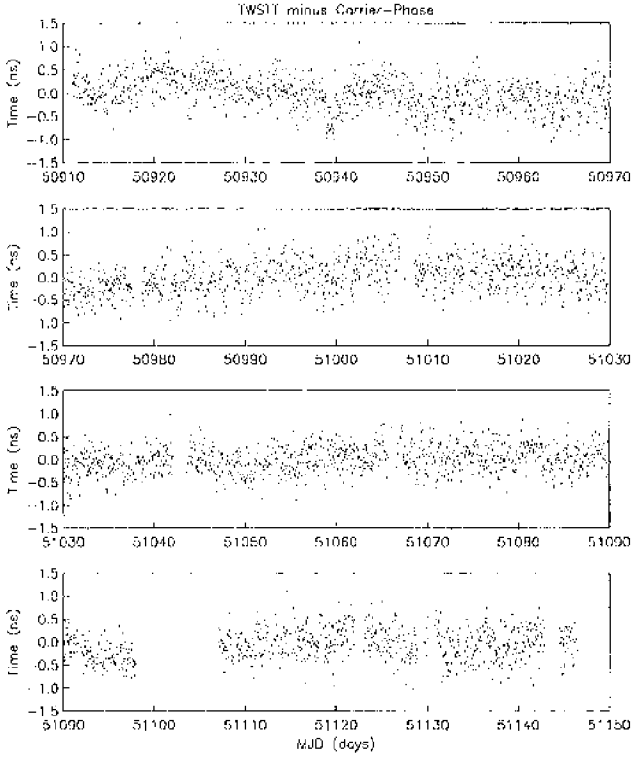

Fig. 5. TWSTT minus carrier-phase clock estimates.

shown at MJD 51 111 [Fig. 6(j); Table II]. Closer inspection of the MC#2-MC#3 hourly data show that MC#2 was steered at that time (as shown in Fig. 7). The carrier-phase data very accurately track this steering. Note that the carrier-phase data were available every 6 min, whereas the local measurements between MC#2-MC#3 and TWSTT are reported hourly. Both the TWSTT and carrier-phase scheme measure differences between AMC#1 and MC#2 (2000 km), whereas the local measurements are over a distance of several hundred meters.

There is another large residual at MJD 50 939 [Fig. 6(a)]. This correlates with a recorded temperature spike in the room where the USNO receiver was kept. Another smaller temperature spike is shown in Fig. 6(b). We can look at these events more closely in Fig. 8. The carrier-phase estimates are showing approximately 200 ps/°C sensitivity to the temperature of the room where the GPS receiver is housed. This is consistent with other work which has shown that clock estimates are sensitive to receiver temperature [4], [10], [16], [20]. In an effort to improve carrier-phase system precision, USNO placed the GPS re-

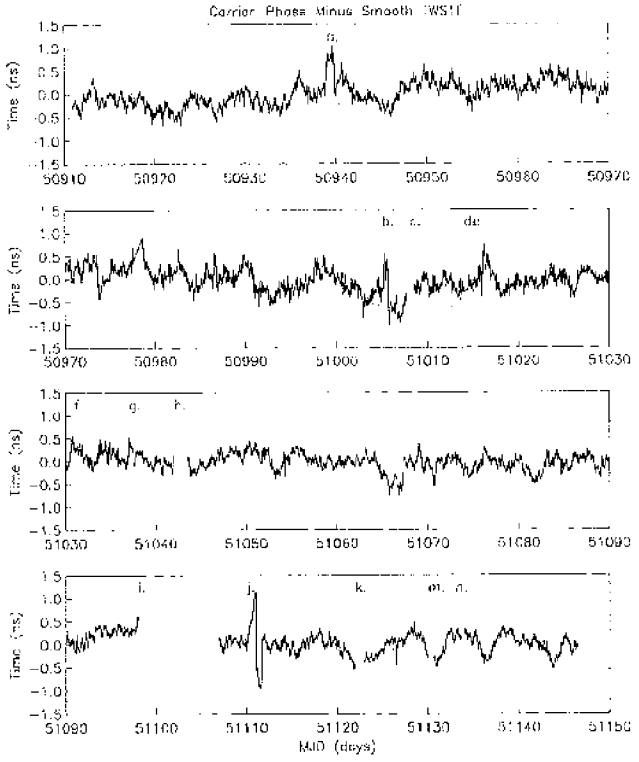

Fig. 6. The difference between carrier-phase clock estimates and smoothed TWSTT. Notes a through n are described in Table II.

ceiver in an isolated thermal chamber on MJD 51 037 [Fig. 6(g)]. This has effectively removed the effects of room temperature on the carrier-phase estimates. Even so, there was a large thermal spike on MJD 51 126 that has affected the carrier-phase estimates [Fig. 6(l)]. Unlike the events shown in Fig. 8, the carrier-phase estimates were negatively rather than positively correlated with temperature and were five times less sensitive to temperature. We believe that at least some of the discrepancy at 51 126 is due to the MC#2-MC#3 calibration data, which shows a marked dependence on temperature.

IX. Carrier-Phase Statistics

The time deviation $\sigma_x(\tau)$, or TDEV [21], is used to quantify the time delay instabilities in time-transfer systems and is related to the modified Allan deviation by the expression

$$\sigma_x(\tau) = \frac{\tau}{\sqrt{3}} Mod\sigma_y(\tau). \tag{3}$$

In computing $\sigma_x(\tau)$ and the Allan deviation, $\sigma_y(\tau)$, we have again restricted our comparison to the first 197 d. In this way, we avoid the 9-d gap in the carrier-phase time series. Because both time series have some unevenly spaced data, we have computed $\sigma_x(\tau)$ and $\sigma_y(\tau)$ using adjacent time values as if they were evenly spaced. We used a τ_o value of 389 and 4644 s, for carrier-phase and TWSTT,

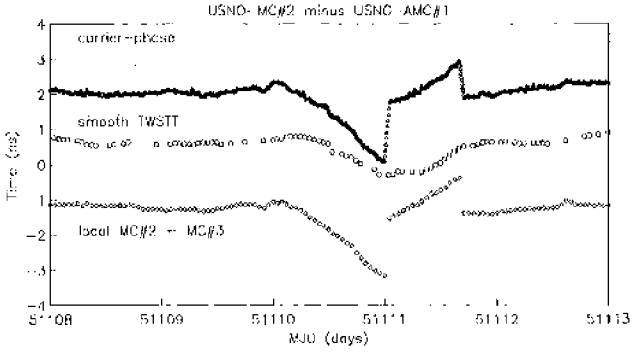

Fig. 7. Carrier-phase (triangles) estimates and smooth Kalman-filtered TWSTT (circles) measurements of USNO-MC#2 - USNO-AMC#1. Also shown are local measurements (diamonds) of USNO MC#2 - MC#3. Data are consistent with local steering records [15].

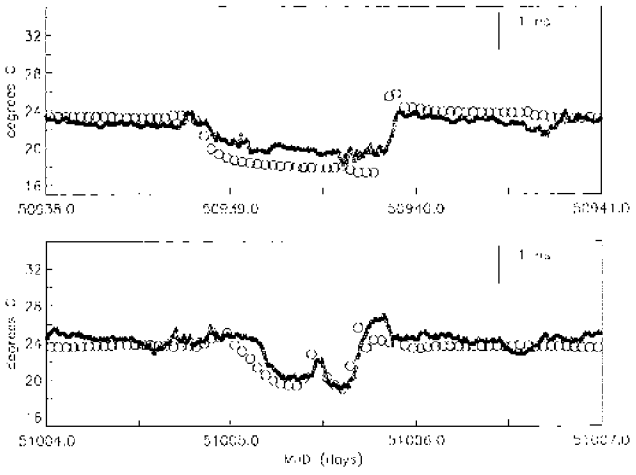

Fig. 8. Hourly temperature records (open circles) for the USNO receiver room plotted along with detrended carrier-phase clock estimates (triangles). The carrier-phase estimates have been converted to °C assuming a conversion relation of 200 ps/°C.

respectively, which is the average measurement time interval between data points.

Fig. 9 summarizes the $\sigma_x(\tau)$ information in the two systems. For periods of less than 1 d, the carrier-phase estimates are significantly more stable than the TWSTT system, with carrier-phase time deviation of 15 to 88 ps between 6 min and 12 h. At approximately 1 d, the two systems overlap in $\sigma_x(\tau)$ and agree for longer periods where clock noise dominates. This is consistent with their long-term agreement in the time domain in Fig. 6. The roll off in time deviation at long time intervals is also consistent with the fact that USNO-AMC#1 is steered to USNO-MC#2. A time series showing the difference of the carrier-phase and TWSTT data (Fig. 5) is particularly useful because it eliminates the clock noise. By calculating $\sigma_x(\tau)$ on this differenced data, the combined instability of the two transfer techniques can be quantified without being corrupted by clock noise. This data in Fig. 9 show that nearly all of the noise at periods less than a day comes from the

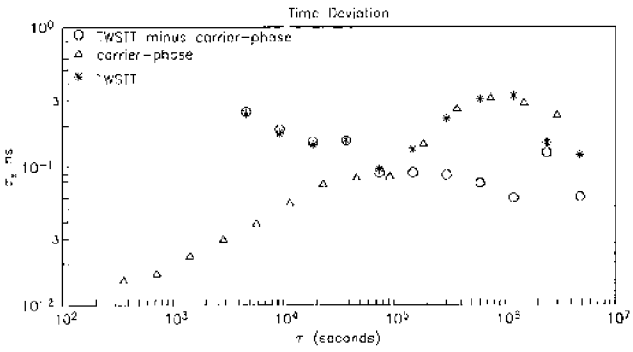

Fig. 9. TDEV of carrier-phase, TWSTT, and the difference between TWSTT and carrier-phase.

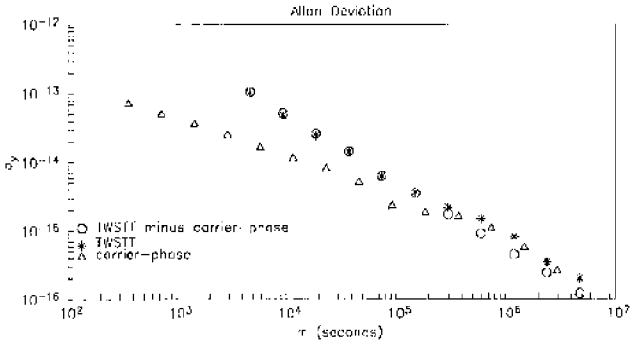

Fig. 10. Allan deviation of carrier-phase, TWSTT, and the difference between TWSTT and carrier-phase.

TWSTT system. In the range of 1 to 30 d, the combined noise of TWSTT and carrier-phase is flicker PM in nature with a level of about 100 ps. A very conservative estimate for the upper limit to the long-term time deviation of carrier-phase can be made by assuming all of the noise is in carrier-phase (this is not very likely). Thus, it can be concluded that $\sigma_x(\tau)$ for carrier-phase using 6-min averages is less than about 100 ps for time intervals from 6 min to 30 d. The Allan deviation plots in Fig. 10 give an indication of the frequency uncertainty of carrier-phase. We see that carrier phase is no worse than 2.5×10^{-15} at 1 d and 8×10^{-16} at 10 d. Unsmoothed TWSTT is 5.5×10^{-15} at one day.

X. Long-Term Stability

As shown in Fig. 7, a carrier-phase system can precisely track clock changes over long distances. Although the agreement between carrier-phase and TWSTT in Fig. 4 is encouraging, we were required to "recalibrate" the carrier-phase estimates with the smooth TWSTT whenever there were significant data outages (all carrier-phase data outages are listed in Table II). Because the USNO-AMCT carrier-phase system was an experimental set-up, it was inevitable that there would be data gaps, equipment changes, and power outages, but this does limit our

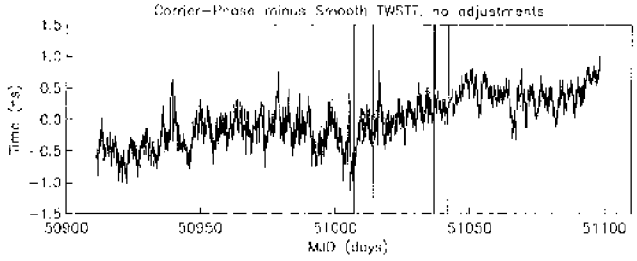

Fig. 11. Carrier-phase estimates minus smooth TWSTT without taking into account data outages in the carrier-phase system. The vertical lines indicate carrier-phase data outages greater than 1-h. These residuals place an upper bound on the long-term stability of this carrier-phase system. The difference between smooth TWSTT and carrier-phase is 5.4 ps/d over 188 d.

ability to study the long-term accuracy of the carrier-phase system. Nonetheless, if we assume that both USNO-AMC#1 and USNO-MC#2 do not drift with respect to each other during these data outages, we will be able to put an upper bound on the errors in the carrier-phase system. In Fig. 11, we show the difference between the "upper-bounded" carrier-phase estimates and the smooth TWSTT data between MJD 50911 to 51098. (We have restricted ourselves to this time period because of the lengthy data outage when new equipment was installed at Schriever.) The agreement between TWSTT and carrier-phase over this period is ±1 ns, with a drift of 5.4 ps/d.

Another source of error that we cannot address with these data is the long-term stability of the MC#3 -MC#2 measurement system. This is currently being studied by USNO. It is believed to be stable to within 1 ns over periods of a year [19]. Note that this uncertainty is comparable with the disagreement mentioned previously.

XI. Prospects for Real-Time Carrier-Phase Time-Transfer

The carrier-phase data used in this study were analyzed after precise IGS orbits were made available on the Internet, 1 to 2 wk after the data from the IGS tracking network were collected. "Rapid" orbits are made available 24 h after the data are collected and, for time-transfer applications at these distances, are nearly as accurate as the precise orbits. The radial precisions for precise and rapid IGS orbits are 3 and 5 cm, respectively [22].

Both the precise and rapid IGS orbit products are computed using GPS carrier-phase data from the global IGS network. To use carrier-phase techniques for time transfer in real time, one will have to use "predicted orbits." These are projections based on the previous day's orbits and will never be as accurate as orbits computed with data. Furthermore, no analysis can predict the behavior of satellites that are maneuvered by the Department of Defense. Even so, if a maneuver is not announced in advance, the satellite can easily be isolated and removed from the solution via

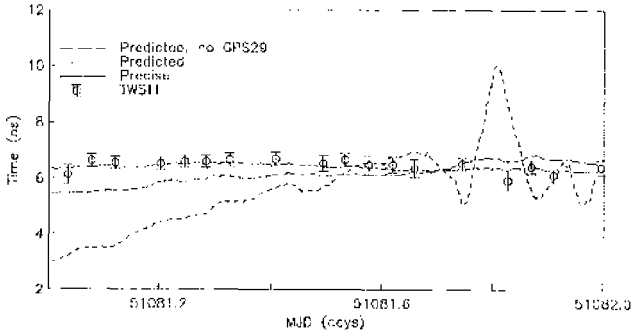

Fig. 12. Carrier-phase clock estimates using precise orbits, predicted orbits (with and without GPS 29), and TWSTT for MJD 51 081. TWSTT measurements are shown with error bars indicating 1 standard deviation.

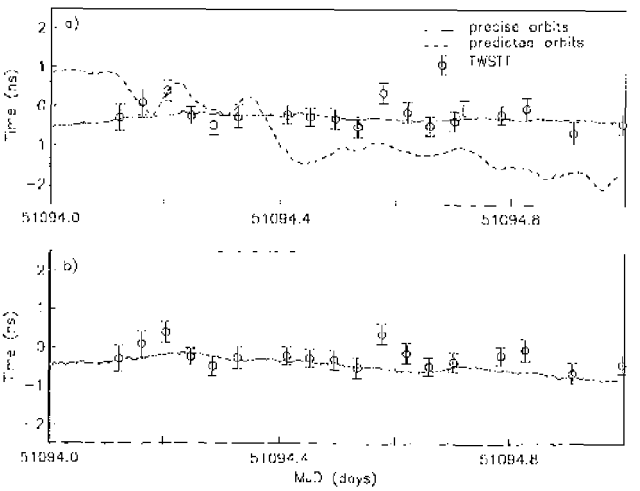

Fig. 13. Carrier-phase clock estimates using (a) precise and predicted orbits and (b) differentially weighted predicted orbits for MJD 51 094. TWSTT measurements are shown with error bars indicating 1 standard deviation.

inspection of post-fit carrier-phase data residuals.

Predicted orbits are produced on a daily basis by the IGS. The projected accuracy for each satellite is also provided in the orbit file, although in practice this information is often neglected. In the absence of such information, each satellite's orbit is assumed to be of the same quality. The accuracy of IGS predicted orbits is partially limited by how quickly the data from the IGS network can be downloaded and made available to the IGS analysis centers that compute the orbits. Originally, data from the IGS tracking network were downloaded once daily. In the last several years, many of the key IGS network sites have upgraded their systems to download their data once hourly. This has been done primarily to support low-Earth-orbiter projects and real-time troposphere studies. With more IGS receivers downloading data on an hourly basis, the IGS expects to see significant improvements in predicted orbit accuracy by the year 2000 [23].

Fig. 12 demonstrates the quality of carrier-phase time-transfer using IGS predicted orbits (MJD 51081). The line shows the carrier-phase estimates with precise orbits, along with TWSTT measurements and their one-standard deviation error bars. We also show clock estimates using predicted orbits for two cases, one which included GPS 29 and one that did not. In the former case, inspection of carrier-phase data residuals (not shown here) clearly demonstrated that the data for GPS 29 were not fit by the model of the orbit. Eliminating GPS 29 improved the fit of the data to the model and also improved the agreement with TWSTT to 1 ns. The predicted orbit uncertainty for MJD 51081 is fairly good with a mean value of 27 cm [24].

In Fig. 13(a), we show carrier-phase time-transfer results using predicted orbits for MJD 51094. As in Fig. 12, we also plot the results using precise orbits and TWSTT. The clock estimates using predicted orbits do not agree with the TWSTT measurements. In this example, we inspected the carrier-phase data residuals, but there was no single outlier satellite, as was seen for MJD 51 081. On this day, the mean orbit uncertainty is 59 cm [25], with extremely poor accuracies for GPS 38, GPS 39, GPS 14, GPS 19, GPS 24, and GPS 25 (138, 115, 125, 371, 221, and 138 cm, respectively). On MJD 51081, we were able to weight the data from all satellites the same; on MJD 51094, it is necessary to weight the satellites differentially to reflect the relative accuracies of the ephemerides. In Fig. 13(b), we show carrier-phase time-transfer estimates using predicted orbits for which we used the accuracy information. Because we have downweighted some of the data, the formal error of the clock estimates double, but the qualitative agreement between the predicted and precise orbit solution has significantly improved.

Further study is required of predicted orbit uncertainty for time-transfer applications, but these examples demonstrate that carrier-phase techniques can be used in real time. Orbit accuracy is crucial to precise carrier-phase time-transfer. Thus, advances in predicted orbit accuracy [23] will continue to improve prospects for real-time carrier-phase time-transfer. Only several minutes of CPU time would be required to analyze the carrier-phase data on an hourly basis.

XII. Conclusions

The high quality TWSTT link between the USNO-AMC#1 and USNO-MC#2 provides a unique opportunity to obtain information about the long-term stability of GPS carrier-phase and TWSTT links.

- The carrier-phase data in the USNO-AMC/USNO-MC link (after temperature correction) have exhibited a stability similar to that observed using the NIST/USNO link reported in [5]. For time intervals less than 1 d, the stability of carrier-phase time-transfer is well below 100 ps.
- High-quality cables should be used for carrier-phase time-transfer experiments, and exposure to the tran-

sient temperature excursions that introduce errors should be minimized by installing the cables within buildings wherever possible.

- Whenever possible, clocks should be connected to the GPS receivers directly to eliminate potential errors in local timing links.
- The carrier-phase receiver should be installed in a thermally controlled chamber.
- Resets of receiver clocks continue to be of concern, although, in this study, simply installing a new receiver diminished the number of resets substantially. Correcting the clock resets with the geodetic receiver we used is simply a matter of finding the nearest integer increment of 24.4427 ns. This technique does not work when the receiver is "rebooted," which is equivalent to a power outage. Ideally the receiver manufacturer should disable the reset capability within the receiver for a timing application user.
- Although further study is required, the carrier-phase technique has demonstrated promising stability for real-time applications using predicted IGS orbits.

XIII. Future Prospects

In this paper, we described the stability of carrier-phase techniques that were developed by the geodetic community. As can be seen from Fig. 9 and 10, an important advantage of the carrier-phase technique over TWSTT is its better noise performance at periods much shorter than 1 d. This advantage is likely to persist qualitatively even when corrections are applied to the calculations in these figures because the data are not exactly equally spaced in time and for the biases that are present in $\sigma_x(\tau)$ at intermediate periods because of the different underlying noise types.

The rough equivalence of the different techniques at longer periods is likely due to the fact that both are limited by the underlying clock noise at these periods. A residual sensitivity to diurnal and other longer period extraneous effects is also quite likely to play a role in both cases -- TWSTT hardware is too large to make temperature control very practical, and there are undoubtedly second-order temperature effects on carrier-phase receivers caused by changes in the impedance in the antenna and the cable that connects it to the receiver.

It is not clear at this time whether this advantage at short periods can be utilized in any effective way because carrier-phase analyses will always require some post-processing. It is certainly true that the mechanical delays in collecting GPS data from the global tracking sites and in analyzing these data to compute orbital parameters can be reduced to some extent. This decrease in the time needed to compute orbital parameters can be combined with automated processing of the data at the timing centers to provide something closer to real-time performance. However, post-processing has an inherent advantage in providing a retrospective look at the data, and that advantage may become less and less significant as the analysis approaches real time.

In the end, the choice between carrier-phase GPS and TWSTT will likely depend on the application and cost. TWSTT may be the method of choice when the data are to be used in a real-time application, such as steering the AMC to the MC. Carrier-phase data are more likely to be used in applications in which the inevitable delays in a retrospective analysis are not important and the fundamental advantages that such an analysis can provide are worth the wait. The better performance of carrier-phase at very short periods may not be the deciding issue in this case. The significant operating costs associated with TWSTT and the case of installing and operating a carrier-phase receiver compared with a TWSTT system may be more important. For example, a carrier-phase receiver costs on the order of $20 000, and there are no additional costs for satellite time as with TWSTT. Carrier-phase analysis costs are the same regardless of the sampling rate.

All of these comments apply only to frequency comparisons. We cannot currently calibrate the effective delay through a carrier-phase GPS receiver in a way that is insensitive to power failures and similar events. This is a result of engineering tradeoffs that were made in the design of these receivers to some extent, but the inherent ambiguities involved in all phase measurements also play a role.

Acknowledgments

This study would not have been possible without many individuals working at USNO. We particularly thank Bill Bollwerk (USNO-AMC), Jim DeYoung (USNO), Steven Hutsell (USNO-AMC), Demetrios Matsakis (USNO), Ed Powers (USNO), and Jim Ray (USNO) for collecting data and for helpful discussions regarding the measurement systems at Schriever AFB and USNO. The GPS receivers at USNO and Schriever are maintained by USNO, and the data are made available through the IGS network. We thank Miranda Chin and Linda Nussear at NOAA for all of their work with the USNO and AMCT receivers. We thank the IGS for providing high quality GPS ephemerides and JPL for software and helpful discussions. We acknowledge computing facilities funded by NASA grant NAG5-6147.

Certain commercial software and equipment are identified in this paper to specify the experimental procedure adequately. Such identification does not imply recommendation or endorsement by the National Institute of Standards and Technology, nor does it imply that the materials or equipment identified are necessarily the best available for the purposes.

References

[1] T. Parker, D. Howe, and M. Weiss, "Making accurate frequency comparisons at the 1×10^{-15} level," in *Proc. 52nd IEEE Int. Freq. Contr. Symp.*, Pasadena, CA, pp. 265–272, 1998.

[2] K. Larson and J. Levine, "Time-transfer using the phase of the GPS carrier," *IEEE Trans. Ultrason., Ferroelect., Freq. Contr.*, vol. 45, no. 3, pp. 539–540, 1998.

[3] P. Baeriswl, T. Schildknecht, J. Utzinger, and G. Beutler, "Frequency and time transfer with geodetic GPS receivers: First results," in *Proc. 9th Eur. Freq. Time Forum*, Besançon, France, pp. 46–51, 1995.

[4] P. Baeriswl, T. Schildknecht, T. Springer, and G. Beutler, "Time-transfer with geodetic GPS receivers using code and phase observations," in *Proc. 10th Eur. Freq. Time Forum*, Brighton, Great Britain, pp. 430–435, 1996.

[5] K. Larson and J. Levine, "Carrier-phase time-transfer," *IEEE Trans. Ultrason., Ferroelect., Freq. Contr.*, vol. 46, no. 4, pp. 1001–1012, 1999.

[6] F. Overney, L. Prost, G. Dudle, Th. Schildknecht, G. Beutler, J. Davis, J. Furlong, and P. Hetzel, "GPS time-transfer using geodetic receivers (GeTT): Results on European baselines," in *Proc. 12th Eur. Freq. Time Forum*, Warsaw, Poland, pp. 94–99, 1998.

[7] Th. Schildknecht and T. Springer, "High precision time and frequency transfer using GPS phase and code measurements," in *Proc. 30th Annu. Precise Time and Time Interval Applications and Planning Mtg.*, Reston, VA, pp. 281–292, 1998.

[8] D. Jefferson, S. Lichten, and L. Young, "A test of precision GPS clock synchronization," in *Proc. 50th IEEE Int. Freq. Contr. Symp.*, Honolulu, HI, pp. 1206–1210, 1996.

[9] G. Petit and C. Thomas, "GPS frequency transfer using carrier phase measurements," in *Proc. 50th IEEE Int. Freq. Contr. Symp.*, Honolulu, HI, pp. 1151–1158, 1996.

[10] G. Petit, C. Thomas, and Z. Jiang, "Use of geodetic GPS Ashtech Z12T receivers for accurate time and frequency comparisons," in *Proc. 52nd IEEE Int. Freq. Contr. Symp.*, Pasadena, CA, pp. 306–314, 1998.

[11] G. Beutler, I. I. Mueller, and R. E. Neilan, "The International GPS service for geodynamics (IGS): Development and start of official service on January 1, 1994," *Bull. Geodesique*, vol. 68, no. 1, pp. 39–70, 1994.

[12] S. Lichten and J. Border, "Strategies for high-precision global positioning system orbit determination," *J. Geophys. Res.*, vol. 92, no. B12, pp. 12,751–12,762, 1987.

[13] J. Zumberge, M. Heflin, D. Jefferson, M. Watkins, and F. Webb, "Precise point positioning for the efficient and robust analysis of GPS data from large networks," *J. Geophys. Res.*, vol. 102, no. B13, pp. 5005–5017, 1997.

[14] P. Koppang and P. Wheeler, "Working application of TWSTT for high precision remote synchronization," in *Proc. 52nd IEEE Int. Freq. Contr. Symp.*, Pasadena, CA, pp. 273–277, 1998.

[15] D. Matsakis, private communication, Jun. 1999.

[16] E. Powers, "Hardware delay measurements and sensitivites in carrier phase time transfer," in *Proc. 30th Annu. Precise Time and Time Interval Applications and Planning Mtg.*, Reston, VA, pp. 293–305, 1998.

[17] L. Young, private communication, Jun. 1998.

[18] K. Larson, L. Nelson, J. Levine, T. Parker, and E. Powers, "A long-term comparison between GPS carrier-phase and two-way satellite time-transfer," in *Proc. 30th Ann. Precise Time and Time Interval Applications and Planning Meeting*, Reston, VA, pp. 247–256, 1998.

[19] E. Powers, private communication, Nov. 1998.

[20] F. Overney, L. Prost, U. Feller, T. Schildknecht, and G. Beutler, "GPS time transfer using geodetic receivers: middle term stability and temperature dependence of the signal delays," in *Proc. 11th Eur. Freq. Time Forum*, Neuchâtel, Switzerland, pp. 504–508, 1997.

[21] D. W. Allan, M. A. Weiss, and J. L. Jespersen, "A frequency-domain view of time-domain characterization of clocks and time and frequency distribution systems," in *Proc. 45th IEEE Freq. Contr. Symp.*, Los Angeles, CA, pp. 667–668, 1991.

[22] J. Kouba and Y. Mireault, "IGS analysis coordinator report," in *IGS 1995 Annual Report*, J. Zumberge, M. Uzban, R. Liu, and R. Neilan, Eds. IGS Central Bureau, Jet Propulsion Laboratory, Pasadena, CA, pp. 45–77, 1996.

[23] G. Gendt, P. Fang, and J. Zumberge, "Moving IGS products towards real-time," in *Proc. 1999 IGS Analysis Center Workshop*, La Jolla, CA.

[24] J. Kouba and Y. Mireault, "Rapid IGS Orbit Prediction Combination - Week 0976, Day 5," *IGS Central Bureau, Jet Propulsion Laboratory*, Pasadena, CA, 1998, pp. 1–2.

[25] , "Rapid IGS Orbit Prediction Combination - Week 0978, Day 4," *IGS Central Bureau, Jet Propulsion Laboratory*, Pasadena, CA, 1998, pp. 1–2.

Kristine Larson was born in Santa Barbara, California, in 1962. She received an A.B. degree in Engineering Sciences from Harvard University in 1985 and a Ph.D. in Geophysics from the Scripps Institution of Oceanography, University of California at San Diego, in 1990. Her dissertation applied the global positioning system to measurements of tectonic motion in the offshore regions of southern California.

From 1988 to 1990, Dr. Larson was also a member of the technical staff of the radiometric tracking division at the Jet Propulsion Laboratory. Since 1990, she has been a faculty member in the Department of Aerospace Engineering Sciences at the University of Colorado at Boulder where she is currently an associate professor. The primary focus of her work is system development of the GPS and applications to measuring plate tectonics, ice flow, plate boundary deformation, volcanic activity, ice mass balance, and time-transfer.

Dr. Larson is a member of the American Geophysical Union.

Judah Levine was born in New York City in 1940. He received a Ph.D. degree in Physics from New York University in 1966. He is currently a physicist in the Time and Frequency Division of the National Institute of Standards and Technology (NIST) in Boulder, Colorado, and is also a Fellow of the Joint Institute for Laboratory Astrophysics, which is operated jointly by NIST and the University of Colorado at Boulder.

He is currently studying new methods for distributing time and frequency information using digital networks such as the Internet and ways of improving satellite-based time and frequency distribution.

Dr. Levine is a Fellow of the American Physical Society and is a member of the American Geophysical Union and the IEEE Computer Society.

Lisa M. Nelson (S'92–S'94–M'96) was born in Denver, Colorado, in 1972. She received her B.S. in 1994 and her M.S. in 1996, both in Electrical Engineering from the University of Colorado. From 1991 until 1994, she was a student research assistant in the Time and Frequency Division at NIST in Boulder, Colorado. Her research was in low-noise systems for measuring frequency stability and accurate phase-noise metrology. Following her graduation in 1994, she joined the staff of the Time and Frequency Division at NIST. She currently works in the Network Synchronization group, where she has primary interest in GPS carrier-phase time-transfer.

Miss Nelson is a member of the Society of Women Engineers, Tau Beta Pi, Eta Kappa Nu, IEEE, and is an EIT. She is also a co-chair of the timing subcommittee of the Civil GPS Service Interface Committee.

Thomas E. Parker (M'79–SM'86–F'94) was born in Natrona Heights, Pennsylvania, in 1945. He received his B.S. in Physics from Allegheny College in 1967. He received his M.S. in 1969 and his Ph.D. in 1973, both in Physics from Purdue University.

In August 1973, Dr. Parker joined the Professional Staff of the Raytheon Research Division, Lexington, Massachusetts. Initially, his work was primarily related to the development of improved temperature-stable surface acoustic wave (SAW) materials. From 1977, Dr. Parker contributed to the development of high performance SAW oscillator technology at the Research Division, including the "All Quartz Package" for SAW devices. His primary interest was frequency stability, with an emphasis on 1/f noise, vibration sensitivity, and long-term frequency stability. In June 1994, Dr. Parker joined the Time and Frequency Division of NIST in Boulder, Colorado. He is the leader of the Atomic Frequency Standards Group, and his interests include primary frequency standards, time scales, and time-transfer technology.

Dr. Parker is a fellow of the IEEE and a member of Sigma Xi and Sigma Pi Sigma. He has served as an elected member of the Administrative Committee of the IEEE Ultrasonics, Ferroelectronics, and Frequency Control Society (1988 to 1990), and as Chair of the Frequency Control Standing Committee of the UFFC-S (1989 to 1997). He has also served on the Technical Program Committees of both the Ultrasonics and the Frequency Control Symposia. He was the Technical Program Committee Chair for the Frequency Control Symposium in 1990 and 1991 and General Chair in 1997 and 1998. Dr. Parker is currently the Associate Editor for Frequency Control-Acoustics of the *UFFC-S Transactions*. Dr. Parker received the 1987 Outstanding Transactions Paper award from the IEEE as a co-author of two papers that appeared in the May 1988 and November 1988 issues of the Transactions. Dr. Parker was the recipient of the Thomas L. Phillips "Excellence in Technology Award" from Raytheon in 1992. In 1994, he received the W.G. Cady Award presented by the IEEE International Frequency Control Symposium. Dr. Parker was the 1996 Distinguished Lecturer of the IEEE Ultrasonics, Ferroelectronics, and Frequency Control Society.